

# Ferroelectric $\pi$ -stacks of molecules with the energy gaps in the sunlight range

Paweł Masiak and Małgorzata Wierzbowska  
*Institute of Physics, Polish Academy of Sciences  
 Aleja Lotników 32/46, PL-02668 Warsaw, Poland*

Ferroelectric  $\pi$ -stacked molecular wires for solar cell applications are theoretically designed, in such a way that their energy gaps fall within visible and infrared range of the Sun radiation. Band engineering is tailored by a modification of the number of the aromatic rings and via a choice of the number and kind of the dipole groups. The electronic structures of molecular wires and the chemical character of the electron-hole pair are analyzed within the density functional theory (DFT) framework and the hybrid DFT approach by means of the B3LYP scheme. Moreover, it is found that one of the advantageous properties of these systems - namely the separate-path electron and hole transport - reported earlier, still holds for the larger molecules, due to the dipole selection rules for the electron-hole generation, which do not allow the lowest optical transitions between the states localized at the same part of the molecule.

## INTRODUCTION

The ability to absorb a wide range of Sun spectrum and convert this energy into the voltage between the electrodes is a key factor of the efficient solar battery. Therefore, the optically active materials ideally should be the composite materials of small-, middle- and wide-bandgap semiconductors, in order to cover the whole radiation range from the soft ultraviolet (350 nm) to the far infrared of a sunset (1400 nm). This possibility is offered by the multilayers of planar molecules or arrays of molecular wires.

Recently, the so-called covalent organic frameworks (COF) attract an attention due to their special optical, transport, and catalytic properties, as well as easy fabrication [1–4]. From a point of view of the photovoltaics, stacks of the COFs are similar to the bulk or integrated heterojunctions [4, 5]. By a change of the planar bonds between the molecules from the covalent to hydrogen bonds, one can restrict the electronic transport to the direction across the layers, i.e. along the stacks, while the electronic transport within the planes shall be suppressed. This is advantageous for the solar batteries, where the planar current would cause only a dissipation of an energy. Therefore, in the previous works [6, 7], we studied the layers of molecules with the COOH terminal groups as the connecting parts for building the networks. The COOH group possesses also a small dipole moment.

The ferroelectrically ordered molecules, composed of benzene rings and two dipole groups (COOH and  $\text{CH}_2\text{CN}$ ), arranged in the  $\pi$ -type stacks of layers or the molecular wires, show many appealing effects [6, 7]. In particular, the energy levels of the subsequent layers (or molecules in a stack) are aligned in a cascade, and this holds for the valence and conduction band as well [6–8]. Each layer is simultaneously a donor and acceptor of electrons and holes, depending on a direction of the carrier motion [6]. The excitons in such layers are localized and have the charge-transfer character from the dipole group to the aromatic central ring. The electric field generated by the ferroelectrically ordered dipole groups leads to a polarization which is induced at electrodes. This effect for the graphene sheets, chosen as the electrodes, causes a change of the work function by  $\pm 1.5$  eV for the anode and cathode, respectively [6]. Moreover, the electrons and holes move across such  $\pi$ -stacks along different paths: the electrons through the central rings and holes between the dipole groups [7]. The carrier mobilities, obtained with the relaxation time estimated due to the elastic scattering and ionic intrusions, are higher than those in the organometal halide perovskites [7, 9, 10]. For all the above reasons, it is interesting to investigate further properties of the ferroelectric molecular layers and stacks, in order to bring these systems closer to the experimental and industrial interest [11].

In this theoretical work, we focus on the rules which govern the bandgap change. The energy gap should fall into an interesting for us range of the Sun radiation. Recently, a similar system (to the cases investigated by us) has been theoretically and experimentally investigated, namely 2D imine polymer [12]. The authors revealed that a bandgap tuning by expanding a conjugation of the backbone of the aromatic diamines is possible in this material [12]. It is also well known that the bandgap decreases with a size of a system [13, 14]. However, without calculations, the exact value of the energy gap is difficult to predict, as well as its dependence on a symmetry and the edge termination [14, 15].

We have begun our study by choosing a type of molecules, which could be most promising for our purpose. Fig. 1 presents some of the molecules which are analyzed in this work. The collection of the geometries of all other studied systems, not presented in figures here, is included in the supporting information. We have chosen three dipole groups: COOH,  $\text{CH}_2\text{CN}$ ,  $\text{CH}_2\text{CF}_3$ , and their combinations in various repetitions. The size of the mesogenic aromatic part was enlarged linearly. The number of the benzene-type rings is given in our notation by an integer number following the "b" letter.

Firstly, we investigated an effect of a number of the aromatic rings and number of dipole groups on a size of the energy gap; it means, the difference between the energetic positions of the lowest unoccupied and the highest occupied molecular orbital (LUMO-HOMO). Secondly, we checked an effect of mixing various chemical groups as the terminal dipoles in one molecule. We estimated also an effect of the  $\pi$ -stacking. Finally, we analyzed how the molecular modifications - which were done in order to tailor the bandgap size - affect the exciton (electron-hole) character and the separation of the charge carrier paths.

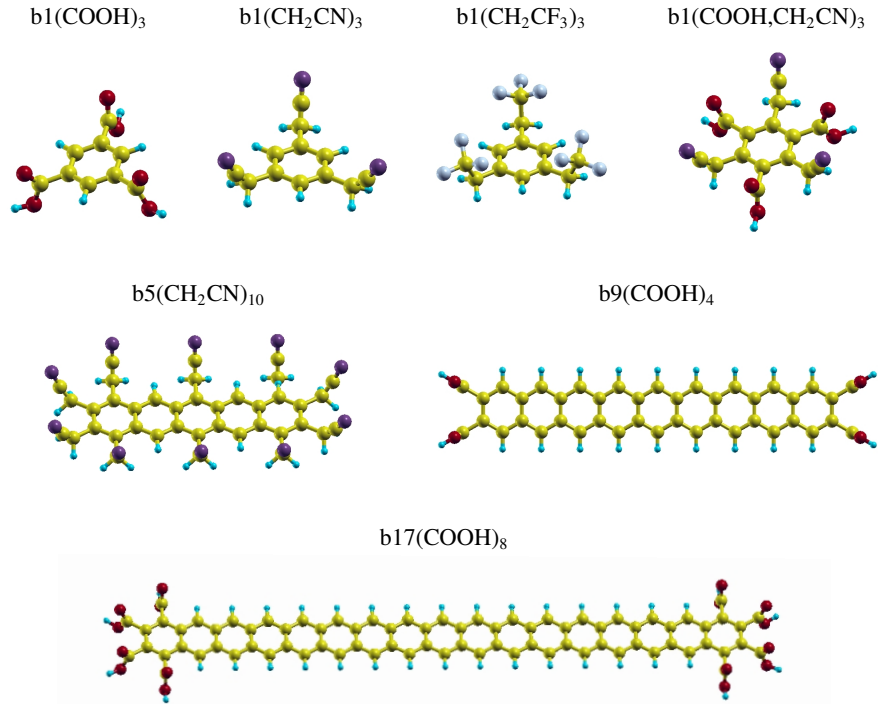


FIG. 1: Atomic structures of some of the studied molecules and their short names.

## THEORETICAL METHODS

The molecular calculations have been performed with the Gaussian code [16], using the correlation-consistent valence double-zeta atomic basis set with polarization function cc-pVDZ [17]. Molecular geometries were optimized with the hybrid-functional method in the B3LYP flavor [18], which mixes the density functional theory (DFT) [19] in the BLYP [20, 21] parametrization with the Hartree-Fock exact exchange in 80% and 20%, respectively. The optimized atomic structures were used to build the molecular wires.

Further calculations for the molecules and 1D structures have been performed with the QUANTUM ESPRESSO suite of codes [22]. This package is based on the plane-wave basis set and the pseudopotentials for the core electrons. The normconserving pseudopotentials were used with the energy cutoff for the plane-waves set to 35 Ry. Moreover, some of the results, such as optimized intermolecular distances, were checked to be the same as using the larger energy cutoff of 45 Ry. The intermolecular distances were obtained within the local density approximation (LDA), since it is known to give better geometries than the generalized gradient approximation (GGA). The LDA-optimized separations between molecules in the stack were then used for the B3LYP calculations for the molecular wires. The uniform Monkhorst-Pack k-points mesh in the Brillouin zone [23] was chosen for  $1 \times 1 \times 10$  for the wires. For the B3LYP scheme, we used the meshes  $1 \times 1 \times 9$  and  $1 \times 1 \times 3$  for the k- and q-point grids, respectively.

In order to obtain the band structures projected onto the local groups of atoms, we employed the wannier90 package [24], which interpolates bands using the maximally-localized Wannier functions [25, 26]. The same tool has been used for the calculations of the dipole moment, which can be obtained from the positions of the maximally-localized Wannier centers,  $r_n$ , using the formula [27]

$$d = \sum_a Z_a R_a - \sum_n r_n \quad (1)$$

where  $Z_a$  and  $R_a$  are the atomic pseudopotential charge and its position, correspondingly, and indexes  $a$  and  $n$  run over the number of atoms and Wannier functions, respectively.

## RESULTS

### Dipole moment

There are a number of important implications of using the dipole groups: i) the hydrogen bonds via the COOH groups within the planes restrict the electronic transport and dissipation of energy in the directions perpendicular to the photovoltaic path, ii) the

polarization generated across the solar device orders the energy levels in a cascade [6], iii) the electronic transport along the  $\pi$ -stacks is restricted to the  $\pi$ -conjugated rings for the electrons, and holes move between the dipole groups [7], iv) an adsorption of the optically active molecules at the surfaces of the transparent conductive oxides, used as the electrodes, leads to the high power conversion when it is realized with the COOH group [28]. Therefore, it is useful to examine various dipole groups for their impact on the energy gaps. In table 1, the dipole moments in the direction parallel to the photovoltaic transport for all studied groups attached to one aromatic ring are collected.

TABLE I: Dipole moment (in Debye) of benzene with chosen polar groups - a component perpendicular to the aromatic ring ( $D_z$ ) - obtained from the LDA calculations and the Wannier-functions spreads according to Eq. 1.

Molecule	$D_z$
b1(COOH) <sub>1</sub>	-0.07
b1(CH <sub>2</sub> CN) <sub>1</sub>	-0.59
b1(CH <sub>2</sub> CF <sub>3</sub> ) <sub>1</sub>	-0.35
b1(COOH,CH <sub>2</sub> CN) <sub>3</sub>	-2.06

### LUMO-HOMO energy differences

A collection of molecules with various lengths of the aromatic chains is gathered in Fig. 2. The energy gaps are presented on a scale of the Sun radiation activity from the soft ultraviolet (350 nm) to the far infrared of a cloudy sky (1400 nm). The impact of various dipole groups on the LUMO-HOMO energy difference does not change with the group types, when they are attached to the long chains (above five benzene rings). Moreover, increasing a number of the dipole groups does not change the energy gap for the longer molecules. Due to the lack of this effect, we can focus on the transport properties when a design of the dipole groups is considered.

It is a well known fact, that the energy gaps obtained with the density functional theory - both in the local density approximation (LDA) and the generalized gradient approximation (GGA) - are underestimated, while the energy gaps from a pure Hartree-Fock method are largely overestimated. Thus, we used the hybrid-functional scheme by means of the B3LYP functional which contains 20% of the exact exchange. The presented series of the energies could be an approximation of the optical gaps - when just a tendency of the size and chemical group effect on the gaps is studied. The experimental data are usually closer to the combined GW+BSE approach taking into account both the quasi-particle and the excitonic binding energy effects [29, 30]. However, from the presented

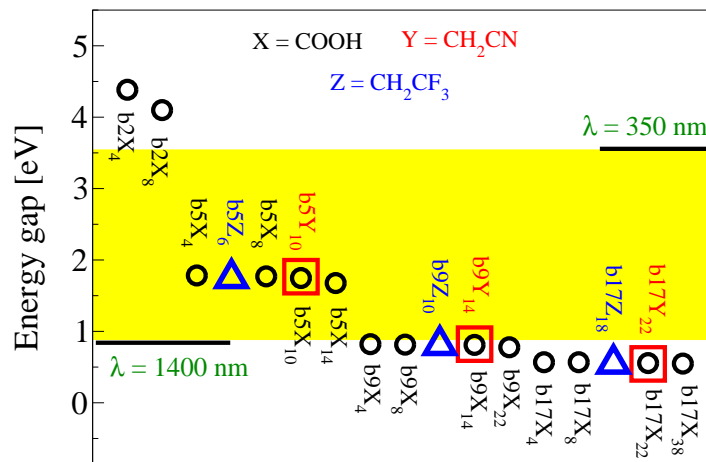


FIG. 2: The LUMO-HOMO energies of the isolated molecules with variable number of benzene rings and three dipole groups: COOH (black circles), CH<sub>2</sub>CN (red squares), CH<sub>2</sub>CF<sub>3</sub> (blue triangles) - obtained with the B3LYP method. The solar spectrum range is marked in yellow. All calculations have been performed with the Gaussian code.

data, it is obvious that a realization of the highly efficient - from the light-absorption point of view - matrices of molecular stacks is possible. Especially, if one combines the layers with columns of various molecules, which have different size and different absorption profiles.

### Impact of the $\pi$ -stacking for the energy gaps

The absorption efficiency is correlated with the thickness of the photoactive layer (Beer-Lambert Law), which cannot be too small making the material to be transparent [31]. Hence, all 2D structures for the solar cells should be examined for their properties across the layers. Stacking causes the band dispersions in the direction perpendicular to the slab. This bandwidth broadening, in turn, acts for the closure of the energy gap. In Table 2, we present an effect of the wire formation on the band gap, and compare the LDA and B3LYP computational methods for chosen systems.

TABLE II: Energy gaps (in eV) of the isolated molecules and molecular wires, obtained with the LDA and B3LYP methods. The last column displays the intermolecular distances (in Å) in the wires (Dist.) - obtained with the LDA scheme and used also for the B3LYP calculations. All calculations have been performed with the QE code.

molecule	$E_{gap}$ (isolated)		$E_{gap}$ (wire)		$\Delta E_{gap}$ (wire-isolated)		Dist. (wire)
	LDA	B3LYP	LDA	B3LYP	LDA	B3LYP	
benzene	5.119	6.717	4.026	5.452	-1.093	-1.265	3.8
b1(COOH) <sub>3</sub>	4.204	6.199	4.037	6.016	-0.167	-0.183	5.1
b1(COOH) <sub>6</sub>	3.956	5.875	3.857	5.813	-0.099	-0.062	5.1
b1(CH <sub>2</sub> CN) <sub>3</sub>	4.293	6.074	3.986	5.692	-0.307	-0.382	4.4
b1(COOH,CH <sub>2</sub> CN) <sub>3</sub>	3.611	5.503	2.963	5.050	-0.648	-0.452	4.6
b1(CH <sub>2</sub> CF <sub>3</sub> ) <sub>3</sub>	4.759	6.359	4.607	6.119	-0.152	-0.239	5.2
b1(COOH,CH <sub>2</sub> CF <sub>3</sub> ) <sub>3</sub>	4.084	5.958	3.946	5.871	-0.138	-0.087	5.2
b1(COOH,CH <sub>2</sub> CN,CH <sub>2</sub> CF <sub>3</sub> ) <sub>1</sub>	4.249	6.196	4.025	5.989	-0.224	-0.207	5.0
b5(COOH) <sub>4</sub>	0.822	1.783	0.738	1.670	-0.084	-0.113	5.1

The last column in Table 2 displays the intermolecular distances obtained with the LDA method. The separation of benzenes, by 3.8 Å, is not much larger than that of the graphene multilayers, which is around 3.4 Å [32]. The most distant are molecules with the CH<sub>2</sub>CF<sub>3</sub> groups, of 5.2 Å. This is due to the fact that they are the largest of all atomic groups attached to the rings studied here, and the F atoms do not attract the H atoms at the bottom of the upper neighbor. The COOH groups are the smallest here, but separations of the molecules terminated by them are also large - of 5.1 Å - because the oxygen atoms from the neighboring rings repel each other. The CH<sub>2</sub>CN groups, although they are also quite large, attract each other between the neighboring rings. This is because N and C tend to "exchange" hydrogen, and this effect leads to the smallest intermolecular distances, of 4.6 Å. The separations of molecules in a wire rule an effect of the bandgap size in the stack; this effect is the strongest for the benzene wires and molecules containing the CH<sub>2</sub>CN groups. It is interesting to note, that an addition of COOH to the rings with other dipole groups weakens an effect of stacking on the band gap. This holds even at the same intermolecular distance (see for instance b1(CH<sub>2</sub>CF<sub>3</sub>)<sub>3</sub> and b1(COOH,CH<sub>2</sub>CF<sub>3</sub>)<sub>3</sub>, or b1(COOH)<sub>3</sub> and b1(COOH)<sub>6</sub> in Table 2). The origin of this effect will be more clear in the next subsection.

Comparison of the LDA and B3LYP approaches for the isolated molecules and wires, usually, exhibits a bit stronger effect of the stacking on the band gap for the hybrid-functional scheme. Also the origin of this effect is similar to that of an addition of COOH, and relies on the order of the energy levels. Because the experimental results for the band gaps of the molecules studied here do not exist yet, it is not easy to determine how good is the B3LYP method in this case. However, one could expect that this method will work similar as in the case of benzene. In order to evaluate effectiveness of the B3LYP method used in our study, we compared energies for benzene calculated by different theoretical methods with experimental result. The energy gap of the benzene molecule (isolated) of 6.72 eV by means of the B3LYP should be compared with the value from the GW approach, of 10.5 eV [33], because both approaches do not take into account the excitonic effects. However, the measured optical gap is around 3.6 eV [34], due to the effect of large exciton binding energy in small molecules. This excitonic effect can be theoretically obtained from the difference of the gaps obtained with the GW and the GW+BSE (BSE means Bethe-Salpeter equation). For benzene, the GW+BSE band gap is around 3.1 eV [30]. Although the B3LYP scheme is much simpler than the GW and GW+BSE methods, and designed for the fundamental gap only, its results are closer to the optical absorption than these of the GW approach. Therefore, we expect that the energy gaps obtained by us with the B3LYP method show the same trends in a series of similar molecules - which differ only with a size or number or type of the dipole groups - as the optical measurements.

### Order of the energy levels

The characters of the highest occupied and lowest unoccupied states determine the excitonic radius and binding energy, the oscillator strength of the absorption of light, as well as the electronic transport properties.

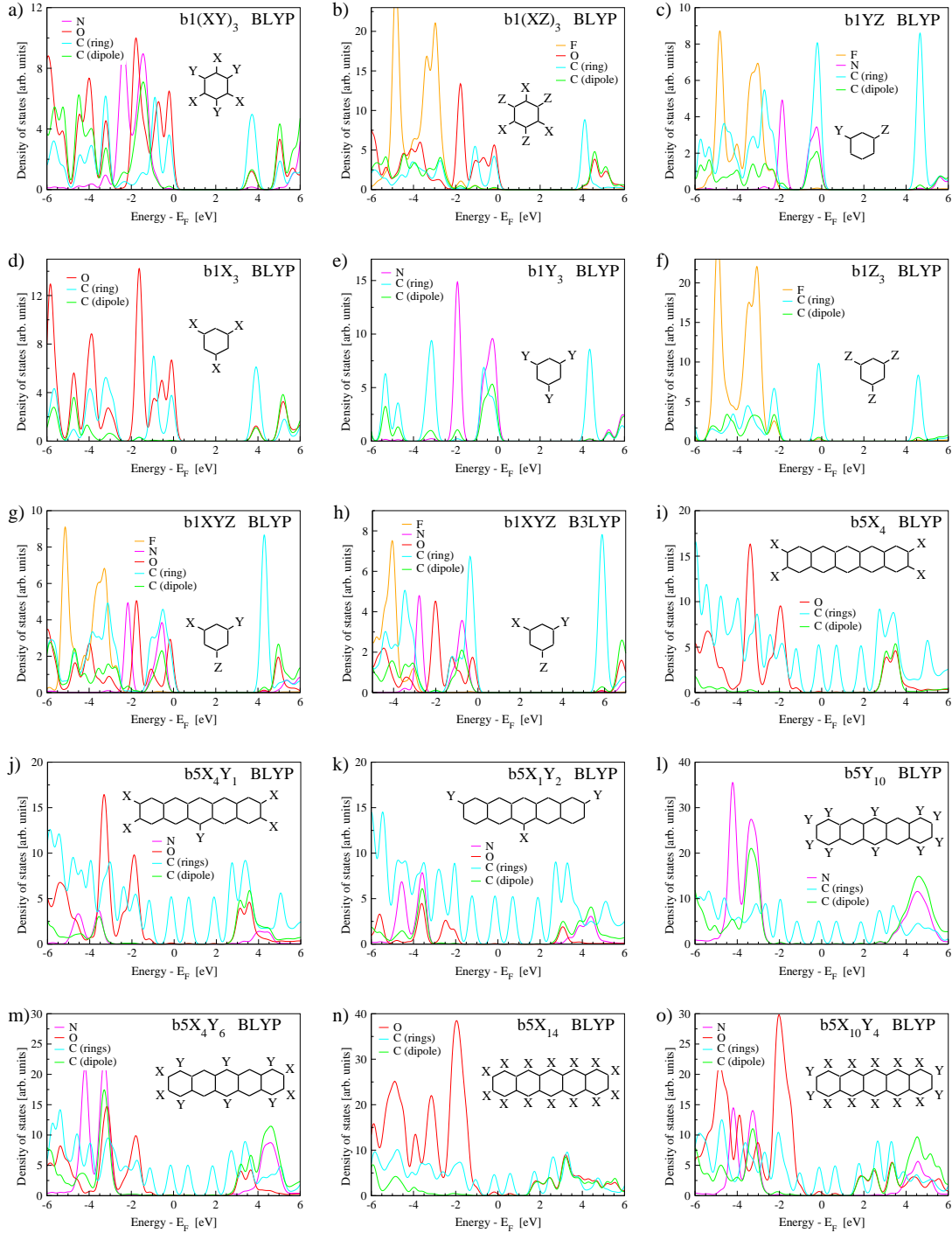


FIG. 3: Density of states (DOS) projected at the atoms of molecules; the systems and methods are denoted within the panels;  $bn$  means a chain of  $n$  benzene rings,  $X=\text{COOH}$ ,  $Y=\text{CH}_2\text{CN}$ ,  $Z=\text{CH}_2\text{CF}_3$ .

In the previous work [7], we showed that one of the systems studied here, namely a wire of  $b1(\text{COOH}, \text{CH}_2\text{CN})_3$  molecules, possesses very localized state at the conduction band minimum (CBM) and the valence band top (VBT). Under the applied voltage, the electrons moved from the central aromatic ring of the molecule to the neighboring ring, while the holes hopped between the

dipole groups. This property might reduce a recombination of carriers and is very desired for solar cell devices [35]. Therefore, we characterize the states around the band gap for the wires composed of some of the  $\pi$ -stacked molecules, studied in this work for their absorption energy. Plots of the projected density of states (PDOS) for wires of benzene and pentacene decorated with various dipole groups are collected in Fig. 3. The choice for the smallest molecule (benzene) is motivated by a need of making a comparison (of the results for the decorated benzene) to our previous studies [7], using the hybrid-DFT method. While the pentacene molecule has been chosen, since it possesses the gap in the sunlight range - and in the same time varying a type and an arrangement of the dipole groups. We varied the type and the arrangement of the dipole groups attached to these molecules in order to check the transport properties. As one will see further, changing the mesogenic part of the molecule does not alter the conclusions.

All results are obtained with the BLYP functional, except for only one case - namely  $b1(\text{COOH}, \text{CH}_2\text{CN}, \text{CH}_2\text{CF}_3)$  - for which the PDOS is calculated also with the B3LYP method. Figs. 3(g) and 3(h) compare these two methods and lead to the following conclusions: 1) The orders of the energy bands are the same - specifically, the O-projected states are close to the Fermi level, and N-projected DOS is deeper in the energy, while the C-ring PDOS is between the O- and N-projected states. 2) The only difference is for the width of the energy band localized at the C-ring - it is more narrow in the B3LYP case and leads to the higher value of the PDOS at the edge of the valence band. Since using the more computationally expensive method does not change the conclusions, we continue with the DFT approach for the PDOS analysis.

When the COOH or  $\text{CH}_2\text{CN}$  dipole groups are attached to a single benzene ring, the highest occupied levels are composed of the states localized at dipoles and partially on the central aromatic ring, while the lowest unoccupied states are built mainly of the C-ring localized orbitals. The oxygen orbitals are closer to the Fermi level than states of the N origin. The fluorine states are the deepest in the energy of all studied dipole groups. Moreover, if only  $\text{CH}_2\text{CF}_3$  groups are attached to benzene then both holes and electrons are predicted to move through the central ring, which is a very unwanted situation. Summarizing results in Figs. 3(a)-(h): the best space separations of the carrier paths are for  $\text{CH}_2\text{CN}$  and COOH. Combinations of these groups work as well. The COOH group is used as a connecting part for the planar structures, as studied in the previous work [6]. It has been demonstrated [28], that using the COOH group for a deposition of the optical material at the transparent electrodes in the solar cell devices one can obtain the highest photovoltaic conversion of all experimentally tested contacts. Thus, only combinations of the COOH and  $\text{CH}_2\text{CN}$  dipoles attached to pentacene molecules are studied further, because they represent the group of molecules which have the energy gaps falling within a convenient range of the Sun spectrum.

In Figs. 3(i)-(o), for each studied case, the highest occupied states of the dipole-group origin are separated from the Fermi level by at least one band. It seems that the carriers separation, found for the decorated benzene in our previous studies [7], may not work very well for larger molecules. However, the PDOS for the dipole localized states is very high, which might cause that the oscillator strength for the absorption is larger than that for the band positioned at the Fermi-level. The calculations of the optical properties by means of the GW+BSE approach are necessary for a full insight. On the other hand, when one builds the planar systems with  $\pi$ -stacking, and adds the electrodes, and applies the voltage - which leads to the Stark shift of the energy levels - then the hole transport between the dipole groups omitting the central aromatic frame might be plausible.

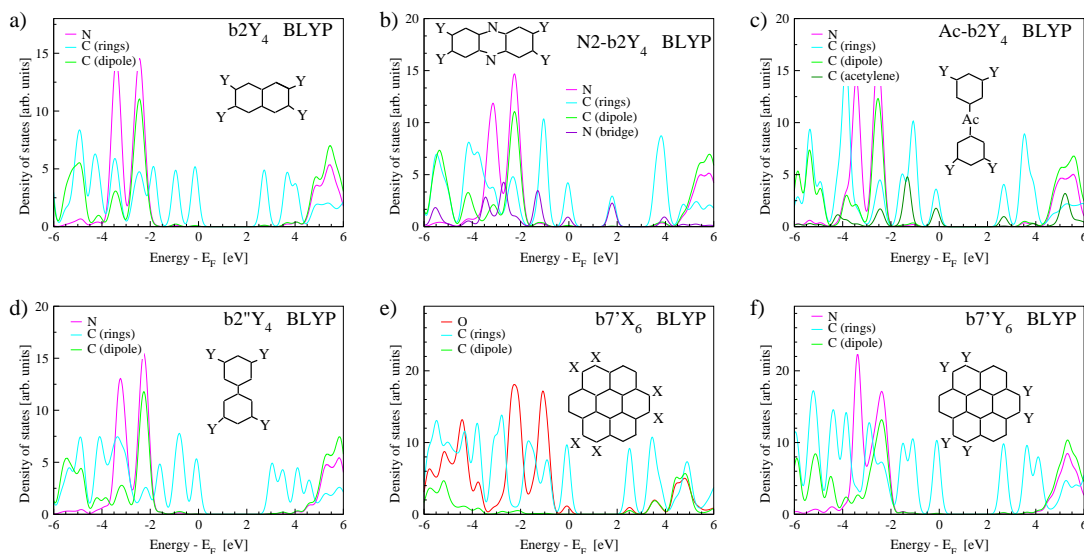


FIG. 4: Density of states (DOS) projected at the atoms of molecules; the systems and methods are denoted within the panels;  $bn$  means a number of benzene rings,  $X=\text{COOH}$ ,  $Y=\text{CH}_2\text{CN}$ , Ac is the acetylene bridge  $-\text{C}\equiv\text{C}-$ . The "prime" and "bis" denote different ways of connecting the aromatic rings or shapes of the aromatic molecular cores.

Additionally, we checked a few more possible connections of two aromatic rings, through: (i) the acetylene (-Ac-), or (ii) nitrogen (-N-) bridges, or (iii) -C-C- bond. The PDOS of naphthalene and bi-phenyl with four  $\text{CH}_2\text{CN}$  groups, and similar systems with the above bridges, are presented in Figs 4(a)-(d). There is only a little improvement of the positioning of the dipole groups in the PDOS, and it is when the -N- bridge is used, with respect to the other possibilities. This means that after an addition of COOH, the light holes will move between the carboxyl groups and the heavy holes between the  $\text{CH}_2\text{CN}$  dipoles, if many terminal groups are attached to the edges. Figs 4(e)-(f) display the projected DOS for the decorated coronene molecule. They confirm earlier findings for the linear aromatic molecules.

As promised earlier in this work, we comment now on the two stacking effects mentioned in the preceding subsection. The strength of the bandgap lowering due to stacking is related to the bands broadening close to the Fermi level. This, in turn, is a function of a strength of the interaction between the neighboring molecules, and of course the distance between them (the closest neighboring groups of atoms are the  $\text{CH}_2$  moieties below the molecular plane and the CN or  $\text{CF}_3$  tops of the dipoles below). Since addition of the COOH group moves the levels of other dipoles down in the energy, the band broadening of these deeper states does not affect so much the energy gap. Therefore, addition of COOH weakens the effect of stacking on the gaps of molecules with  $\text{CH}_2\text{CN}$  or  $\text{CH}_2\text{CF}_3$  dipoles. In the same way, the B3LYP method - which lowers a contribution of the dipole-group projected DOS at the Fermi level with respect to the BLYP - leads to a smaller stacking effect on the band gap. The latest effect is due to the fact that, the C-ring states of the neighboring molecules originate from the groups of atoms, which are more distant than the neighboring dipoles in the stack.

#### Absorption spectra of three molecules in a series of the growing size of the mesogenic part

At the end, we compare the theoretical absorption spectra for a series of three molecules with growing number of benzene rings in a chain, i.e. 2, 5 and 9, but having the same number and type of the dipole groups, namely four COOH moieties attached on the both sides of the longer molecular axis, as in Fig. 1 for  $\text{b9}(\text{COOH})_4$  (i.g.  $\text{b9X}_4$ ) and in Fig. 3(i) for  $\text{b5X}_4$ . These spectra are simulated with the Yambo code [36], using its possibility to calculate the dielectric function. The response function was obtained on the random phase approximation level. In Fig. 5, both the interacting ( $\text{Im } \epsilon$ ) and noninteracting ( $\text{Im } \epsilon_0$ ) dielectric functions show the blue shift of the dominant absorption peaks with the growing molecular size.

The imaginary part of the noninteracting dielectric functions have the absorption edges at the energies which correspond to the DFT energy gaps - which are: 2.99 eV for  $\text{b2X}_4$ , 0.84 eV for  $\text{b5X}_4$ , and 0.04 eV for  $\text{b9X}_4$ . Measured absorbance is more similar with the interacting dielectric function, which has the prominent peaks between 2 and 4 eV for  $\text{b5X}_4$  and  $\text{b9X}_4$ , and between 4 and 6 eV for  $\text{b2X}_4$ . The GW+BSE spectrum would be shifted up due to the many-body effects and down due to the excitonic effects. Nevertheless, our main message that it is possible to tune the optical spectra of the dipole decorated molecules in the  $\pi$ -stacks is still valid.

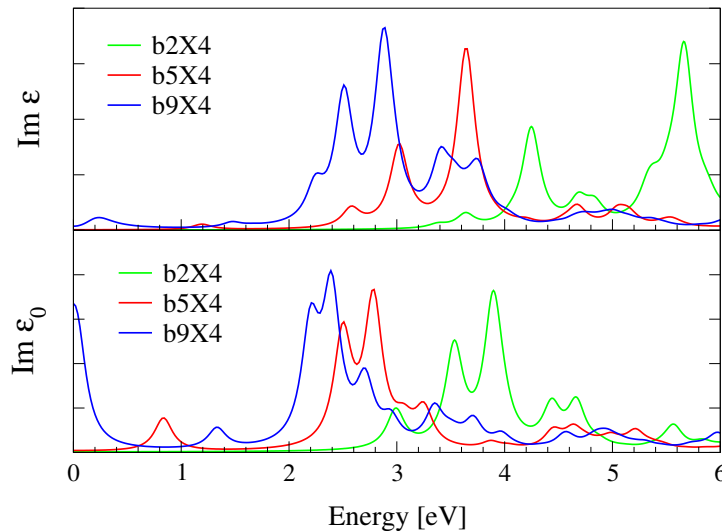


FIG. 5: The imaginary part of the interacting (top panel) and noninteracting (bottom panel) dielectric function for three chosen molecules, obtained with the Yambo code.



The second optimistic message is connected to the transport properties, which are correlated with the oscillator strength of the dipole optical transitions and creation of the electron-hole pairs. As we see from the interacting dielectric function, the lowest absorption peak is much higher in the energy than the HOMO-LUMO gap. This means that the optical transitions between the DOS peaks which are the most close to the Fermi level (on its occupied and unoccupied sides) are not allowed. These peaks were of the same origin, namely they were localized at the central C-rings and not the dipole groups. Instead, the higher energetic positions of the first absorption peaks in these molecules suggest that the allowed transitions are between the C-rings and dipole groups. This is a wanted property, because the electron-hole pairs will be generated on the spatially distant parts of the molecule. Thus, we retain the space separation of the charge transport for electrons and holes again, for the larger molecules than benzene.

## CONCLUSIONS

Our aim is to tailor the band gap in the molecular  $\pi$ -stacks, in order to propose systems - with ferroelectric properties investigated earlier [6, 7] - for the solar cell applications. Tuning the optical properties is possible by varying a number the benzene rings and a choice of the dipole groups when the molecules are small. While in cases of larger molecules, with longer aromatic chains, the band gaps are almost independent on the terminal groups. On the other hand, a choice of the dipole groups and their number are critical parameters for the atomic localization of the highest occupied and lowest unoccupied states. Therefore, the character of the photogenerated electron-hole pair is sensitive to the chemical connections between the neighboring molecules in the stacks and this, in turn, determines the transport properties [7].

Summarizing: the linear chains, between five and nine of the aromatic rings, are good candidates for building blocks of the organic nanostructures for photovoltaic applications, when they are terminated with the COOH and CH<sub>2</sub>CN groups. While using the CH<sub>2</sub>CF<sub>3</sub> groups does not give the desired properties. The dipole selection rules for the optical transitions retain the charge-paths selectivity, which appears to be lost when looking just at the PDOS.

## ACKNOWLEDGEMENT

This work has been supported by The National Science Centre of Poland (the Project No. 2013/11/B/ST3/04041). Calculations have been performed in the Cyfronet Computer Centre using Prometheus computer which is a part of the PL-Grid Infrastructure, and by part in the Interdisciplinary Centre of Mathematical and Computer Modeling (ICM).

- 
- [1] Cook TR, Yang RY, Stang PJ (2013) Metal-Organic Frameworks and Self-Assembled Supramolecular Coordination Complexes: Comparing and Contrasting the Design, Synthesis and Functionality of Metal-Organic Materials. *Chem Rev* 113(1):734-777
  - [2] Chakrabarty R, Mukherjee PS, Stang PJ (2011) Supramolecular Coordination: Self-Assembly of Finite Two- and Three-Dimensional Ensembles. *Chem Rev* 111(11):6810-6918
  - [3] Medina DD, Rotter JM, Hu Y, Dogru M, Werner V, Auras F, Markiewicz JT, Knochel P, Bein T (2015) Room temperature synthesis of covalent-organic framework films through vapor-assisted conversion. *J Am Chem Soc* 137(3):1016-1019
  - [4] Calik M, Auras F, Salonen LM, Bader K, Grill I, Handloser M, Medina DD, Dogru M, Löbermann F, Trauner D, Hartschuh A, Bein T (2014) Extraction of photogenerated electrons and holes from a covalent organic framework integrated heterojunction. *J Am Chem Soc* 136(51):17802-17807
  - [5] Xiao Z, Yuan Y, Yang B, VanDerslice J, Chen J, Dyck O, Duscher G, Huang J (2014) Universal formation of compositionally graded bulk heterojunction for efficiency enhancement in organic photovoltaics. *Adv Mater* 26(19):3068-3075
  - [6] Wierzbowska M, Wawrzyniak-Adamczewska M (2016) Cascade donoracceptor organic ferroelectric layers, between graphene sheets, for solar cell applications. *RSC Adv* 6, 49988-49994
  - [7] Wawrzyniak-Adamczewska M, Wierzbowska M (2016) Separate-Path Electron and Hole Transport Across -Stacked Ferroelectrics for Photovoltaic Applications. *J Phys Chem C* 120(14), 7748-7756
  - [8] Sobolewski AL (2015) Organic photovoltaics without p-n junctions: a computational study of ferroelectric columnar molecular clusters. *Phys Chem Chem Phys* 17(32):20580-20587
  - [9] Motta C, El-Mellouhi F, Sanvito S (2015) Charge carrier mobility in hybrid halide perovskites. *Sci Rep* 5:12746(1)-12746(8)
  - [10] Leijtens T1, Stranks SD, Eperon GE, Lindblad R, Johansson EM, McPherson IJ, Rensmo H, Ball JM, Lee MM, Snaith HJ (2014) Electronic properties of meso-superstructured and planar organometal halide perovskite films: charge trapping, photodoping, and carrier mobility. *ACS Nano* 8(7):7147-7155
  - [11] Zhao YS, Fu H, Peng A, Ma Y, Xiao D, Yao J (2008) Low-Dimensional Nanomaterials Based on Small Organic Molecules: Preparation and Optoelectronic Properties. *Adv Mater* 20(15):2859-2876



- [12] Xu L, Yu Y, Lin J, Zhou X, Tian WQ, Nieckarz D, Szabelski P, Lei S (2016) On-surface synthesis of two-dimensional imine polymers with a tunable band gap: a combined STM, DFT and Monte Carlo investigation. *Nanoscale* 8(16):8568-8574
- [13] Deng JP, Chen WH, Chiu SP, Lin CH, Wang BC (2014) Edge-termination and core-modification effects of hexagonal nanosheet graphene. *Molecules* 19(2):2361-2373
- [14] Hu W, Lin L, Yang C, Yang J (2014) Electronic structure and aromaticity of large-scale hexagonal graphene nanoflakes. *J Chem Phys* 141(21):214704(1)-214704(10)
- [15] Singh SK, Neek-Amal M, Peeters FM (2014) Electronic properties of graphene nano-flakes: energy gap, permanent dipole, termination effect, and Raman spectroscopy. *J Chem Phys* 140(7):074304(1)-074304(9)
- [16] Frisch MJ et al. (2013) Gaussian 09, Revision D.01. Gaussian, Inc., Wallingford CT
- [17] Dunning Jr TH (1989) Gaussian Basis Sets for Use in Correlated Molecular Calculations. I. The Atoms Boron Through Neon and Hydrogen. *J Chem Phys* 90(2):1007-1023
- [18] Becke AD (1993) Density-functional thermochemistry. III. The role of exact exchange. *J Chem Phys* 98(7):5648-5652
- [19] Kohn W, Sham LJ (1965) Self-Consistent Equations Including Exchange and Correlation Effects. *Phys Rev.* 140(4A):A1133-A1138
- [20] Becke AD (1988) Density-functional exchange-energy approximation with correct asymptotic behavior. *Phys Rev A*, 38(6):3098-3100
- [21] Lee C, Yang W, Parr RG (1988) Development of the Colle-Salvetti correlation-energy formula into a functional of the electron density. *Phys Rev B* 37(2):785-789
- [22] Giannozzi P, Baroni S, Bonini N, Calandra M, Car R, Cavazzoni C, et al. (2009) QUANTUM ESPRESSO: a modular and open-source software project for quantum simulations of materials. *J Phys Condens Matter* 21(39):395502(1)-395502(19)
- [23] Monkhorst HJ, Pack JD (1976) Special points for Brillouin-zone integrations. *Phys Rev B* 13(12):5188-5192
- [24] Mostofi AA, Yates JR, Lee YS, Souza I, Vanderbilt D, Marzari N (2008) wannier90: A tool for obtaining maximally-localised Wannier functions. *Comput Phys Commun* 178:685-699
- [25] Marzari N, Vanderbilt D (1997) Maximally localized generalized Wannier functions for composite energy bands. *Phys Rev B* 56(20):12847-12865
- [26] Marzari N, Mostofi AA, Yates JR, Souza I, Vanderbilt D (2012) Maximally localized Wannier functions: Theory and applications. *Rev Mod Phys* 84(4):1419-1475
- [27] Resta R (1994) Macroscopic polarization in crystalline dielectrics: the geometric phase approach. *Rev Mod Phys* 66(3):899-915
- [28] Manoharan S, Asiri AM, Anandan S (2016) Impact of anchoring groups for improving the binding nature of organic dyes toward high efficient dye sensitized solar cells. *Solar Energy* 126:22-31
- [29] van Setten MJ, Caruso F, Sharifzadeh S, Ren X, Scheffler M, Liu F, Lischner J, Lin L, Deslippe JR, Louie SG, Yang C, Weigend F, Neaton JB, Evers F, Rinke P (2015) GW100: Benchmarking G0W0 for Molecular Systems. *J Chem Theory Comput* 11(12):5665-5687
- [30] Blase X, Attaccalite C (2011) Charge-transfer excitations in molecular donor-acceptor complexes within the many-body Bethe-Salpeter approach. *Appl Phys Lett* 99(17):171909(1)-171909(3)
- [31] Lee J-Y, Tsai M-C, Chen P-C, Chen T-T, Chan K-L, Lee C-Y, Lee R-K (2015) Thickness Effects on Light Absorption and Scattering for Nanoparticles in the Shape of Hollow Spheres. *J Phys Chem C* 119(46):25754-25760
- [32] Borysiuk J, Sołtys J, Piechota J (2011) Stacking sequence dependence of graphene layers on SiC (0001) - Experimental and theoretical investigation. *J Appl Phys* 109(9):093523(1)-093523(6)
- [33] Neaton JB, Hybertsen MS, Louie SG (2006) Renormalization of Molecular Electronic Levels at Metal-Molecule Interfaces. *Phys Rev Lett* 97(21):216405(1)-216405(4)
- [34] Hanazaki IJ (1972) Vapor-phase electron donor-acceptor complexes of tetracyanoethylene and of sulfur dioxide. *J Phys Chem* 76(14):1982-1989
- [35] Wehrenfennig C, Eperon GE, Johnston MB, Snaith HJ, Herz LM (2014) High Charge Carrier Mobilities and Lifetimes in Organolead Trihalide Perovskites. *Adv Mater* 26(10):1584-1589
- [36] Marini A, Hogan C, Grüning M, Varsano D (2009) YAMBO: an *ab initio* tool for excited state calculations. *Comp Phys Comm* 180:1392-1403

## SUPPLEMENTARY INFORMATION

TABLE I: Numerical data set for Fig. 2: the LUMO-HOMO energies (in eV) of the isolated molecules with variable number of benzene rings and three dipole groups:  $X=\text{COOH}$ ,  $Y=\text{CH}_2\text{CN}$ ,  $Z=\text{CH}_2\text{CF}_3$ .

b2X <sub>4</sub>	b2X <sub>8</sub>	b5X <sub>4</sub>	b5Z <sub>6</sub>	b5X <sub>8</sub>	b5Y <sub>10</sub>	b5X <sub>10</sub>	b5X <sub>14</sub>	b9X <sub>4</sub>	b9X <sub>8</sub>
4.384	4.099	1.783	1.745	1.770	1.766	1.748	1.677	0.820	0.814
b9Z <sub>10</sub>	b9Y <sub>14</sub>	b9X <sub>14</sub>	b9X <sub>22</sub>	b17X <sub>4</sub>	b17X <sub>8</sub>	b17Z <sub>18</sub>	b17X <sub>22</sub>	b17Y <sub>22</sub>	b17X <sub>38</sub>
0.808	0.821	0.810	0.778	0.568	0.568	0.547	0.556	0.544	0.549

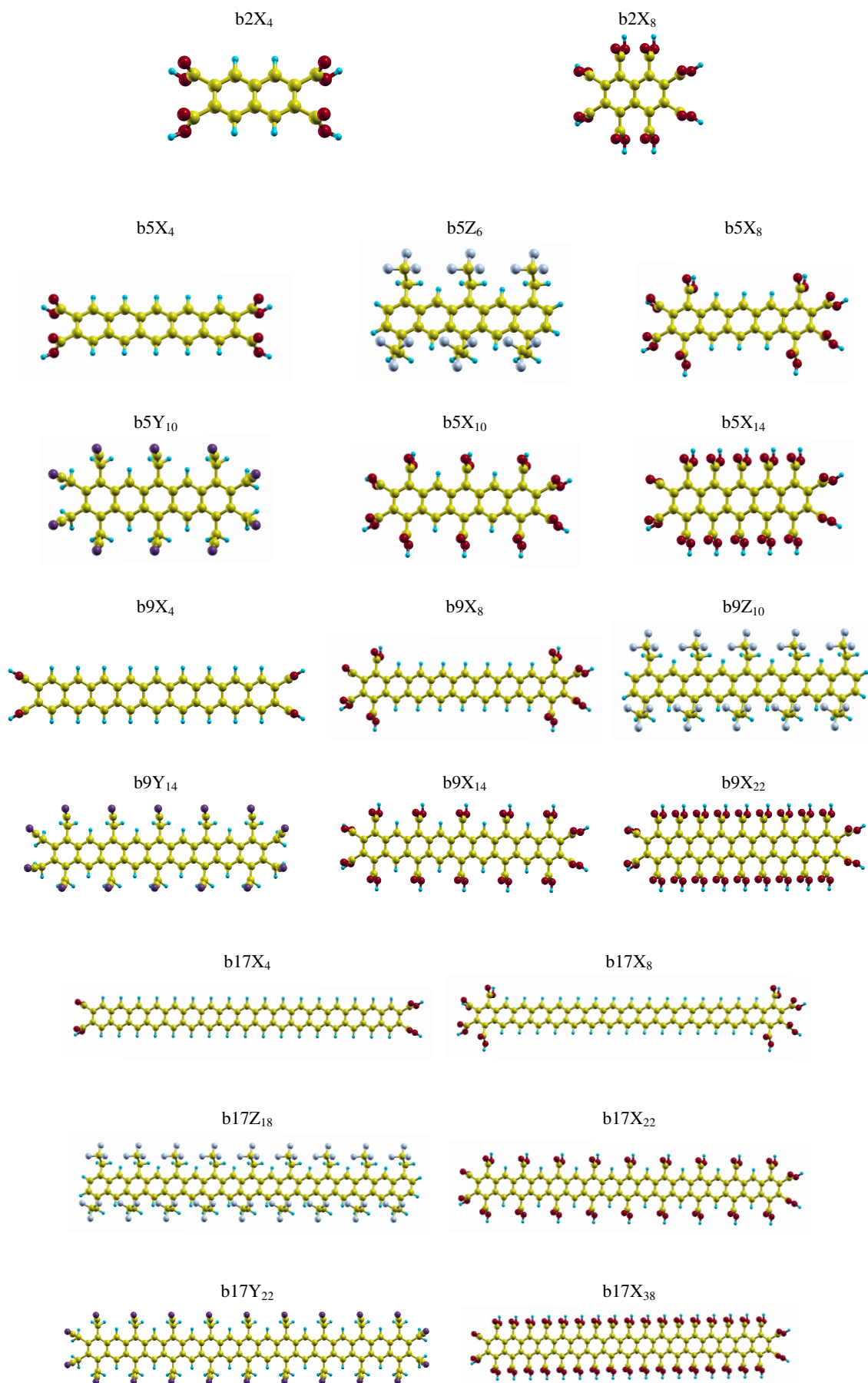


FIG. 1: Atomic structures of molecules for which the LUMO-HOMO gaps are presented in Figure 2.

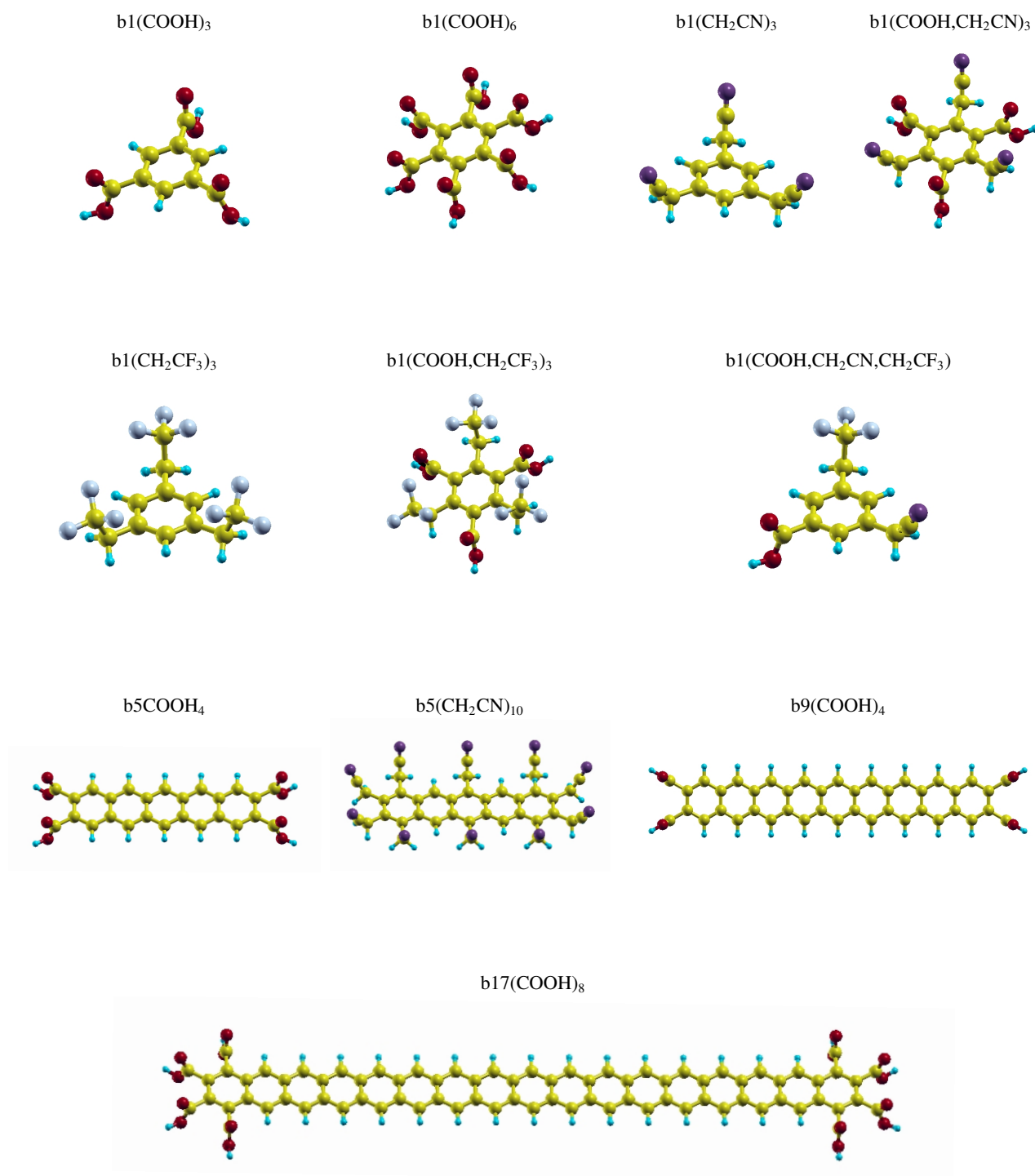


FIG. 2: Atomic structures of molecules mentioned in Table 2 of the paper.